


Article

Incident Angle Dependent Formation of Ion Tracks in Quartz Crystal with C_{60}^+ Ions: Big Ions in Small Channels

Hiroshi Amekura ^{1,*} , Kazumasa Narumi ², Atsuya Chiba ², Yoshimi Hirano ², Keisuke Yamada ², Shunya Yamamoto ² and Yuichi Saitoh ²

¹ National Institute for Materials Science (NIMS), Tsukuba 305-0003, Japan

² National Institutes for Quantum Science and Technology (QST), Takasaki 370-1292, Japan; narumi.kazumasa@qst.go.jp (K.N.); chiba.atsuya@qst.go.jp (A.C.); hirano.yoshimi@qst.go.jp (Y.H.); yamada.keisuke@qst.go.jp (K.Y.); yamamoto.shunya@qst.go.jp (S.Y.); saito.yuichi@qst.go.jp (Y.S.)

* Correspondence: amekura.hiroshi@nims.go.jp; Tel.: +81-29-863-5479

Abstract: Quartz (SiO_2) crystals possess intrinsic columnar pores perpendicular to (0001) surfaces, consisting of three- and six-membered ring (3MR and 6MR) structures of Si and O atoms. The diameters of the larger pores, i.e., 6 MRs, are ~ 0.49 nm, while the diameters of fullerene (C_{60}) ions are 0.7 nm, i.e., larger than either type of the pores. Transmission electron microscopy observation evidenced approximately two times longer ion tracks in the channeling condition, i.e., 0° incidence to (0001) surface, than an off-channeling condition, i.e., 7° incidence in this case, under 6 MeV C_{60} ion injection. The track length at the 0° incidence decreases more steeply than that at the 7° incidence with decreasing the energy from 6 MeV to 1 MeV. Finally, the track lengths at the 0° and 7° incidences become comparable, i.e., the channeling-like effect disappears at 1 MeV irradiation. This study experimentally indicates that the channeling-like effect of C_{60} ions is induced in quartz crystals, while the sizes of the channels are smaller than the C_{60} ions.

Keywords: channeling; ion track; C_{60} ion; quartz; six-membered ring



Citation: Amekura, H.; Narumi, K.; Chiba, A.; Hirano, Y.; Yamada, K.; Yamamoto, S.; Saitoh, Y. Incident Angle Dependent Formation of Ion Tracks in Quartz Crystal with C_{60}^+ Ions: Big Ions in Small Channels. *Quantum Beam Sci.* **2022**, *6*, 4. <https://doi.org/10.3390/qubs6010004>

Academic Editor: Lorenzo Giuffrida

Received: 27 August 2021

Accepted: 7 January 2022

Published: 12 January 2022

Publisher's Note: MDPI stays neutral with regard to jurisdictional claims in published maps and institutional affiliations.



Copyright: © 2022 by the authors. Licensee MDPI, Basel, Switzerland. This article is an open access article distributed under the terms and conditions of the Creative Commons Attribution (CC BY) license (<https://creativecommons.org/licenses/by/4.0/>).

1. Introduction

When an ion is injected into a crystal along some special directions, the ion range is drastically extended compared to the random incidence. This phenomenon is called “ion channeling”, and is utilized for broad applications of ion beams, including analyses [1]. However, the channeling of cluster ions in solids has an intrinsic limitation—as the sizes of the channels are determined from the lattice structures and the geometry between the ion beam and the crystals, and much larger channels than the usual ones are not easily attained, particularly in inorganic solids. On the other hand, the sizes of cluster ions can be more easily enlarged. Consequently, we may encounter situations where the sizes of the projectiles are larger than any of the channels in a solid.

Figure 1a schematically depicts atomic structures of the low temperature phase (trigonal) of quartz crystal (SiO_2), looking from the $\langle 0001 \rangle$ direction. As shown in Figure 1a, the (0001) plane of the quartz consists of three-membered rings (3MRs) and six-membered rings (6MRs), which are composed of three pairs and six pairs of Si-O atoms, respectively. While the cross-section of 6MR is not circles but dodecagons, distance between diagonal Si pairs of 0.4916 nm gives an approximate diameter for the 6MR pores. In Figure 1a, a fullerene (C_{60}) ion, with a diameter of 0.7 nm, is also depicted in the same scale as the (0001) plane of quartz. From the geometrical constraints, it looks impossible for a C_{60} ion to enter the quartz crystal from the $\langle 0001 \rangle$ direction without destructing the crystal structures of quartz and/or the C_{60} molecule itself. In fact, C_{60} molecules are broken to fragments inside of solids via collisions between constituent atoms in the solid and constituent C atoms in C_{60} molecules, or via Coulomb repulsions between ionized C atoms in C_{60} molecules [2].

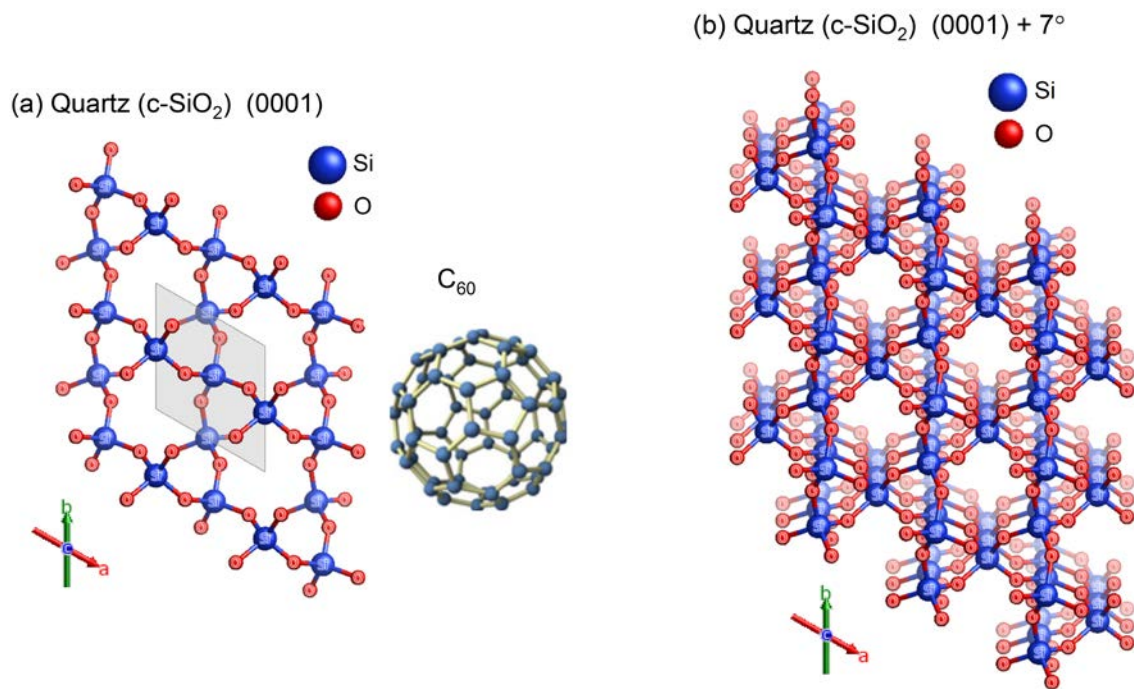


Figure 1. (a) Schematically depicted atomic structures of the low temperature phase of quartz (SiO₂) crystal looking from the $\langle 0001 \rangle$ direction. ReciPro software [3] was applied for plotting. Large and small pores (channels) are extended along the $\langle 0001 \rangle$ direction, which consist of six-membered rings (6MRs) and three-membered rings (3MRs) of Si and O atoms, respectively. A C₆₀ ion is depicted in the same scale with the (0001) plane of the quartz. (b) The (0001) plane is tilted by 7°. While only three layers are depicted, the channels of 3MRs are almost closed. The channels of 6MRs are also closed with an additional two or three layers.

Figure 1b exhibits the crystal structures of quartz looking from the direction of 7°-tilted from the $\langle 0001 \rangle$ direction. While only three atomic layers are depicted, the channels of 3MRs are almost closed. Those of 6MRs are still open by half. However, with additional plots of two or three layers, the 6MR channels are also closed. Therefore, tilting of 7° corresponds to an off-channeling condition.

In this paper, the lengths of ion tracks in quartz crystal formed by the 1–6 MeV C₆₀ ion irradiations were evaluated by transmission electron microscopy (TEM) observations and were compared between two different incident angles of 0° (channeling condition) and 7° (off-channeling condition). There are a huge number of reports on ion irradiation effects in crystalline quartz [4–15]. Here, ion track formation in quartz is reported, where the ion tracks are damaged regions of cylindrical shapes induced by irradiations of swift heavy ions (SHI) or cluster ions [16,17]. The ion tracks in crystalline quartz induced with SHI irradiation have been extensively studied [7,11–14]. In addition, the track formation with C₆₀ cluster ion irradiation has been studied [2,18–22]. Recently, Amekura et al. reported track formation in crystalline quartz [23] and crystalline silicon [24] using several MeV C₆₀ ion irradiation. As each of single C₆₀ ion deposited a huge energy along its trajectory, the observation of ion tracks by TEM corresponds to the observation of the trajectory of each single C₆₀ ion. However, the tracks are not recorded when the C₆₀ energy decreases below the threshold or when the C₆₀ ion is fragmented into much smaller parts.

The conventional channeling of monomer ions is well described by the continuum model proposed by Lindhard [25]. In the case of the monomer ions, there is enough space to change the trajectories freely in the channels. Interacting with the atomic rows around the channel, the ion traverses almost the center of the channel, where core electrons from the surrounding atom rows cannot reach. Furthermore, nuclear collisions between the channeling ions and the surrounding atoms seldom occur. However, in the case of C₆₀ ions,

the 6 MR channel is fully occupied by many simultaneously injected C atoms. This situation is much different from the channeling of the monomer ions. Because of the geometrical restriction of the many simultaneously injected C atoms, certain C atoms may stay in the center of the channel where the interaction is rather weak, but the other many C atoms are pushed close to the surrounding atomic rows. The latter atoms are suffered by strong interactions not only with the core electrons, but by the nuclear collisions with atomic rows around the channels. Furthermore, as the 6MR channel is smaller than the C_{60} ion, a certain portion of C atoms from a C_{60} molecule cannot enter the same 6MR channel and inject into neighboring 6MRs and/or 3MRs. In addition, these atoms may be suffered by nuclear collisions. Therefore, the present phenomenon, i.e., the transport of C_{60} ions, which strongly depends on the incident angle of the C_{60} ions, is not exactly the same as the channeling of the monomer ions. Here, we call the present phenomenon the channeling-like effect.

2. Materials and Methods

Samples of $3\text{ mm} \times 4\text{ mm} \times 0.5\text{ mm}$ were mechanically cut from commercially available z-cut quartz (SiO_2) single crystals. The faces of $3\text{ mm} \times 4\text{ mm}$, which are parallel to the (0001) plane, were irradiated with C_{60}^+ ions with an incident angle of 0° or 7° from the surface normal. The irradiation of C_{60}^+ ions was conducted at the Takasaki Advanced Radiation Research Institute (TARRI) of the National Institutes for Quantum Science and Technology (QST) using a 3 MV tandem accelerator with proper charge-exchanger gas [26] and a newly developed high-flux C_{60} negative ion source [27]. The samples were irradiated at one of the energies of 1, 2, 3, 4 and 6 MeV, to a fluence between 5×10^{10} and 5×10^{11} C_{60}/cm^2 . For precise control of the low fluences, the ion flux was reduced to a few-tens of pA through mesh-type attenuators and an aperture of 3 mm in diameter, while using the high-flux ion source.

After irradiation, a thin Pt layer was deposited on the irradiated surface of the sample as a surface marker for cross-sectional TEM observation. Then, the samples were thinned down to a thickness of $\sim 100\text{ nm}$ for electron beam transmission by using 30 keV Ga^+ focused ion beam (FIB) milling. TEM observation was conducted using JEOL JEM-2100 and JEM-2100F microscopes with an operation voltage of 200 kV. The samples were irradiated with five different energies of C_{60} ions between 1 and 6 MeV at the two different incident angles of 0° and 7° , i.e., at nine different conditions. An image of only one TEM sample with 4 MeV irradiation of 7° incidence has been published in a previous paper [23].

3. Experimental Results

Figure 2 shows bright field cross-sectional TEM images of quartz crystals irradiated with 6 MeV C_{60} ions, with an incident angle of (a) 0° and (b) 7° from the surface normal. The black thin layer in each image is a Pt layer deposited for the surface marker. Many thin cylindrical structures are observed in Figure 2b at the bulk side of the Pt layer, which are ion tracks. We have already reported in [23] the ion track formation in crystalline quartz under 4 MeV C_{60} ion irradiation with an incident angle of 7° . In addition, the hillock formation has been reported in [23]. While we showed a TEM image irradiated with 4 MeV C_{60} ions of 7° incidence in the previous paper, here, similar hillocks were observed in the image irradiated with 6 MeV C_{60} ions of 7° incidence, as shown in Figure 2b. The incident angle dependence has never been reported anywhere before.

A thick layer at the vacuum side of the Pt layer is a deposited carbon layer for supporting against the FIB milling. At the normal incidence (a), a surface damage zone which does not show any tracks inside is observed between the bottom side of the Pt layer and the track layer where many tracks are observed. While many crystalline TEM samples change the image contrast with small tilting, the surface damage zones do not change the contrast. Therefore, we consider that the zone is amorphous or highly damaged. At the 7° incidence (b), the surface damage zone was not observed, or it was very thin if it even existed. However, this is not a common feature. In some cases, thicker surface damage zones were observed even at the 7° incidence.

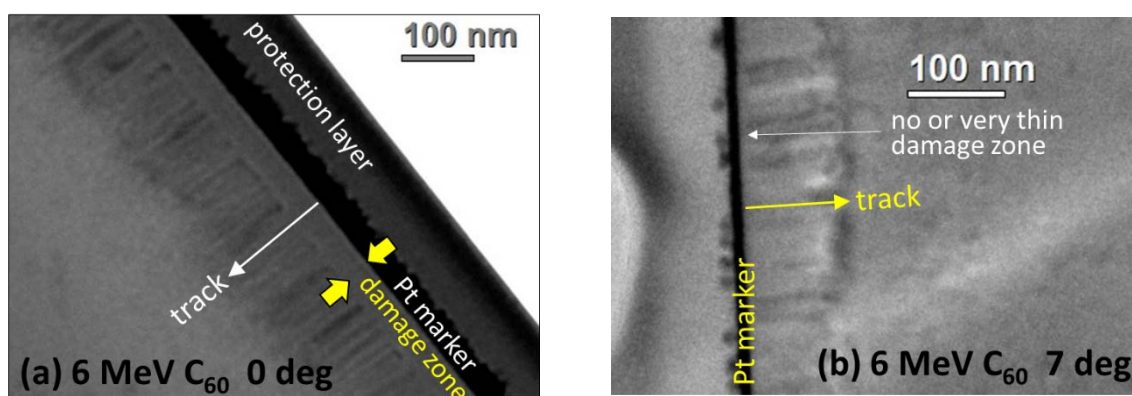


Figure 2. Cross-sectional TEM images of quartz irradiated with 6 MeV C_{60}^+ ions to a fluence of $5 \times 10^{11} C_{60}^+/\text{cm}^2$. The incident angle of the C_{60} ions was set to (a) 0° and (b) 7° from the surface normal. Black thin layers are Pt layers deposited on the surface markers. In (a), a surface damage zone without showing any tracks is observed between the black thin layer of deposited Pt (surface marker) and the track layer where a lot of tracks are observed. In (b), the track layer was observed just below the Pt layer without the surface damage zone. In (b), many black dots are observed on the Pt layer, which could be ascribed to Pt deposited on hillocks.

In Figure 2b, many black dots are observed at the vacuum side of the Pt layer. Judging from the contrast of the image, the dots themselves are made of Pt. Maybe hillocks were formed on the surface of the quartz sample by C_{60} irradiation, and they were covered by deposited Pt with mostly maintaining their shapes. As the Pt layer was thicker by accident in the 0° incidence sample (a), fine information of the irradiated surface could be washed out. While the image in Figure 2b was irradiated with 6 MeV C_{60} ions, a similar image was also reported under 4 MeV C_{60} irradiation in our previous paper [23].

In order to determine the mean track length, we made the following assumption: The tracks are formed even inside of the surface damage zone, while they are not visible because of the amorphous or strongly damaged nature of the damage zone. Observation of ion tracks by TEM requires crystallinity of the matrix materials. While the tracks are observed in quartz, i.e., a crystalline form of SiO_2 [7,13], they are not possible in amorphous SiO_2 [28]. The disappearance of the ion tracks in quartz crystal with the amorphization is reported in the supplementary material of Ref. [23]. Here, we define the length of the tracks as the distance from the bottom of the Pt layer to the tails of the tracks, including the thickness of the insensitive layer. In this definition, the mean track length of the 0° incidence was 202 ± 30 nm under 6 MeV C_{60} irradiation, roughly double of the length of the 7° incidence of 124 ± 19 nm. The ion energy dependences of the track length are plotted for the two different incident angles of 0° and 7° in Figure 3a. The results at 4 MeV were qualitatively the same with those at 6 MeV, except for a decrease in the mean track length. The mean length under 4 MeV irradiation decreased to 153 ± 23 nm at the 0° incidence, which was still double of the length at the 7° incidence, i.e., 87 ± 13 nm.

Figure 3a clearly indicates that the track length clearly decreased with changing the incident angle from 0° to 7° at the same energies. This behavior is regarded as the channeling-like effect of C_{60} ions through the quartz crystal, while the 6MRs and 3MRs of quartz were smaller than the diameters of C_{60} ions.

With decreasing the energy of the incident C_{60} ions as shown in Figure 3, the track length of the 0° incidence decreased more steeply than that of the 7° incidence. Consequently, the length difference between the 0° and the 7° incidences decreased with decreasing the C_{60} energy. At 1 MeV C_{60} irradiation, the track length of the 0° incidence and that of the 7° incidence become comparable within experimental error.

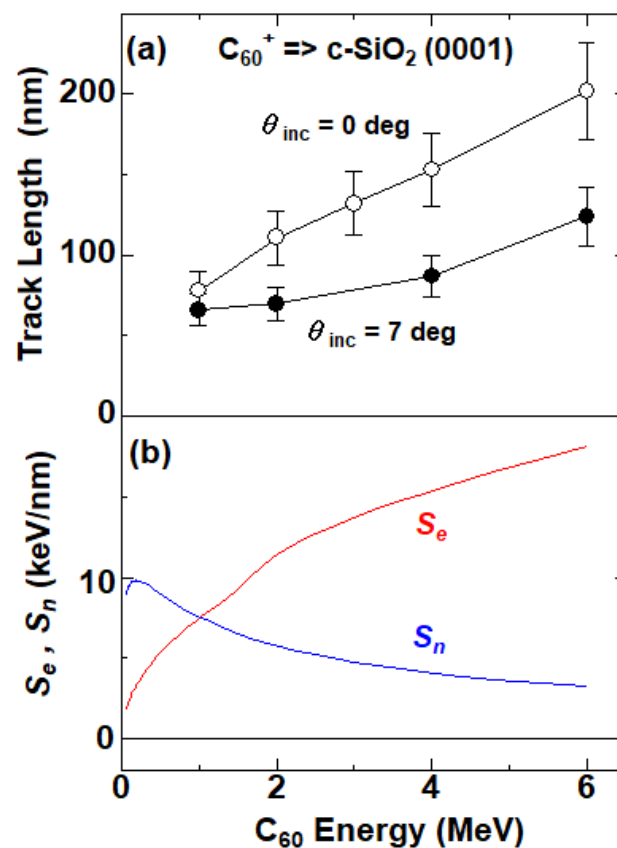


Figure 3. Ion energy dependence of (a) the mean track length at the 0° (open circles) and 7° (closed circles) incidences from the surface normal of the (0001) surface of quartz crystal, and of (b) electronic and nuclear stopping powers (S_e and S_n) of C_{60} ions in quartz.

The energy dependence of the electronic and nuclear stopping powers (S_e and S_n) of C_{60} ions was estimated from the relation [29,30]:

$$S_i(E, C_{60}) = N \cdot S_i(E/N, C_1) \quad (1)$$

where $i = e$ (electronic) or $i = n$ (nuclear), and $N = 60$ is presumed for C_{60} ions. The stopping powers of the monomer ions $S_i(E, C_1)$ were calculated with SRIM 2013 [31]. With decreasing the C_{60} energy from 6 MeV to 1 MeV, S_e decreases but S_n increases. S_e was greater than S_n at 2 MeV or higher, where the channeling-like effect was observed. On the contrary, S_e was comparable to S_n at 1 MeV where the track length was comparable between the 0° and 7° incidences.

The assumption of $N = 60$ in Equation (1) is rigorously valid only when the interaction between each C constituent is negligible. This is not the case for the C_{60} ion, where 60 C atoms are injected simultaneously to the size of the C_{60} molecule, i.e., a radius of 0.7 nm. A strong enhancement or reduction was expected. However, the experiments reported that the approximation of $N \sim 60$ was not so bad. Recently, Kaneko et al. calculated the electronic stopping power of a C_{60} ion in electron gas, with assuming that the shape and the size of C_{60} did not change, and derived the value of N . While the value of N weakly depends on the energy, it is approximately reduced as $N/60 \sim 0.8$, i.e., $N \sim 50$, between 2 MeV and 10 MeV [32]. We instead considered that the calculated factor of 0.8 was very close to unity, indicating that the approximation of $N \sim 60$ was not so bad.

While the energy dependence of the track length was weaker for the 7° incidence, as shown in Figure 3a, similar weak energy dependence was also observed in crystalline silicon irradiated with 1–6 MeV C_{60}^+ ions with an incident angle of 7° [24].

4. Discussion

4.1. Surface Damage Zone

Currently, we have no idea about the formation processes of the surface damage zones. First of all, ion fluence of $5 \times 10^{11} \text{ C}_{60}/\text{cm}^2$ was applied to the samples, which is too low to overlap the tracks to form a continuous amorphous layer.

The thickness of the damaged zones ranged from nearly zero to ~50 nm, depending on the sample. Contrarily, the range of C_{60} ion with energy E after fragmentation could be roughly approximated by the range of monoatomic C ion with energy $E/60$. Following this approximation, the ranges of 4 MeV and 6 MeV C_{60} ions were estimated from SRIM 2013 [31] as 280 nm and 400 nm, respectively, both of which were much deeper than the thickness of the damage zones. Therefore, conventional amorphization due to the accumulation of track overlaps was excluded.

Furthermore, even two TEM samples that were prepared under almost the same conditions exhibited quite different thicknesses of the damage zones. It was speculated that the thickness of the damage zone was determined not by the irradiation conditions of C_{60} ions, but possibly by the fabrication processes or the observation processes of the TEM samples. It should be noted that quartz has a high susceptibility for amorphization. In fact, as reported in the Supplementary Materials in Ref. [23], we observed a crystalline-amorphous transition of quartz during TEM observation. Sample surfaces or deposited metal layers could be seeds for amorphization, particularly under electron or focused ion beam irradiations. The damage zones are always observed at the bottom of the Pt layers, when they do exist.

In addition, prolonged TEM observation could increase the thickness of the damage zones. We also tried observations using a scanning TEM (STEM) JEM-2100F, which irradiated the sample with a much higher electron flux, and we observed a drastic increase in damage zone thickness. Under the conventional bright field observation by JEM-2100, we did not notice changes in the thickness of the damage zone during the observations. However, slow changes cannot be excluded.

4.2. Factors Governing the Track Length

To discuss the ion penetration of C_{60} ions in solids, the dissociation processes of C_{60} molecules should be taken into account. When a C_{60} molecular ion is injected into a solid, the C_{60} molecule is no longer stable due to two effects [2]. The first one is the repulsive forces between the ionized C constituents, as each C atom forming a C_{60} molecule is suffered by ionization once the C_{60} ion is injected into a solid. Because of the repulsive Coulombic force between each C constituent, the C_{60} molecule expands until it is regarded as 60 independent C ions. The second effect is the nuclear collisions between constituent atoms of the target material and carbon atoms of C_{60} molecule. This process leads loss of carbon atoms from the C_{60} molecule, which finally results in the fragmentation of the C_{60} molecules. For C_{60} ions of a few tens of MeV or lower, the latter process is reported to be dominant [2]. Because of these two processes, C_{60} ions tend to break down to smaller fragments or monomers, unless they cease moving before the break down. In fact, the branching of ion tracks of C_{60} ions is reported, e.g., in YIG crystals [2].

Track formation with C_{60} ions is also a complicated process. While the diameter of a C_{60} molecule is 0.7 nm, the track diameter of 4 MeV C_{60} ions in quartz is ~10 nm [23]. The energy transport from the C_{60} ion at the center of the track (0.35 nm) to the entire body of the track (~5 nm) is governed via δ -electrons emitted from the C_{60} ion. The inside of the track is heated up with the δ -electrons and electron cascades of lower energies. The track diameter depends on the electronic energy deposition S_e (and the ion velocity). There is a S_e threshold, below which tracks are no longer formed. The S_e threshold of quartz is known as the velocity dependent, as 2 keV/nm and 4 keV/nm for 0.5 MeV/u and 7 MeV/u, respectively [13]. Because of low velocities of C_{60} ions (in the order of 0.001 MeV/u), a threshold of 2 keV/nm was adapted for the present study.

The electronic energy loss S_e of the C_{60} ion was estimated from Equation (1) with the help of SRIM2013. The S_e of 6 MeV C_{60} was derived as 18.1 keV/nm in quartz, which is much higher than the track formation threshold of 2 keV/nm. Consequently, track formation was expected. However, if a C_{60} ion with an initial energy of 6 MeV is dissociated into 60 independent carbon monomer ions, each C monomer receives the energy of 100 keV = 6 MeV/60 on average. The S_e of the C monomer ion of 100 keV amounts to 0.30 keV/nm in quartz, which is far below the threshold of 2 keV/nm. Therefore, the track formation by a single C monomer is not expected. To generate a track in quartz, seven or more C atoms ($0.30 \text{ keV/nm} \times 7 \text{ atoms} = 2.1 \text{ keV/nm} > 2 \text{ keV/nm}$) should form a carbon cluster. An expected, but confusing, behavior is that the fragmented cluster ions, i.e., C_p and C_q ($p, q < 60$), could additively contribute to track formation, if both the cluster ions traverse while maintaining themselves within a certain distance.

5. Conclusions

Ion energy dependence of the ion track formation in z-cut quartz single crystals (SiO_2) with C_{60} ions at the energies between 1 and 6 MeV were evaluated by TEM observations at two different incident angles of the channeling condition (0° from the surface normal) and the off-channeling condition (7°). A thin Pt layer was deposited for each sample after C_{60} ion irradiation as a surface marker. The surface damage zones, which show insensitive contrast with tilting and are probably ascribed to amorphous or strongly damaged regions, were observed between the Pt layer and the track-dominant layer.

We analyzed the data under an assumption where ion tracks were formed, even inside of the damage zones, but the tracks were not visible because of the amorphous or strongly-damaged nature of the zones. Approximately twice longer ion tracks were formed at the 0° incidence than at the 7° incidence under 6 MeV C_{60}^+ irradiation. This observation indicates that the channeling-like effect is induced in quartz with MeV C_{60} ions, while the sizes of C_{60} ions was larger than the pore sizes of the quartz (0001) surface.

With decreasing the energy of the incident C_{60} ions from 6 MeV to 1 MeV, the track length at the 0° incidence decreased more steeply than that of the 7° incidence. Consequently, the length difference between the 0° and 7° incidences decreased. At 1 MeV irradiation, the track lengths of the 0° incidence and 7° incidence became comparable. Therefore, the channeling-like effect almost disappeared around 1 MeV.

Author Contributions: Conceptualization, H.A. and K.N.; sample preparation, H.A.; C_{60} beam developments and irradiation, A.C., Y.H., K.Y., S.Y., K.N. and Y.S.; TEM observation, H.A.; manuscript preparation, H.A. All authors have read and agreed to the published version of the manuscript.

Funding: This research received no external funding.

Data Availability Statement: The datasets and materials generated during the current study are available from the corresponding author on reasonable request.

Acknowledgments: A part of the study was supported by the Inter-organizational Atomic Energy Research Program through an academic collaborative agreement among JAEA, QST, and the University of Tokyo. The authors are grateful to the crew of the accelerator facilities at QST-Takasaki for their help. TEM observation was performed using the facility of the NIMS TEM station.

Conflicts of Interest: The authors declare no conflict of interest.

References

1. Chu, W.-K.; Mayer, J.W.; Nicolet, M.-A. *Backscattering Spectrometry*; Academic Press New York: New York, NY, USA, 1978.
2. Dunlop, A.; Jaskierowicz, G.; Jensen, J.; Della-Negra, S. Track separation due to dissociation of MeV C_{60} inside a solid. *Nucl. Instrum. Methods Phys. Res. Sect. B Beam Interact. Mater. At.* **1997**, *132*, 93.
3. Seto, Y. ReciPro, ver. 4.791. Available online: <https://github.com/seto77/ReciPro> (accessed on 6 January 2022).
4. Primak, W. Radiation-induced stress relaxation in Quartz and vitreous silica. *J. Appl. Phys.* **1964**, *35*, 1342.
5. Chandler, P.J.; Zhang, L.; Townsend, P.D. High temperature annealing of He^+ ion-implanted quartz optical waveguides. *Nucl. Instrum. Methods Phys. Res. Sect. B Beam Interact. Mater. At.* **1990**, *46*, 69.

6. King, B.V.; Kelly, J.C.; Dalglish, R.L. Stress and strain in quartz and silica irradiated with light ions. *Nucl. Instrum. Methods Phys. Res.* **1983**, *209–210*, 1135.
7. Meftah, A.; Brisard, F.; Costantini, J.M.; Dooryhee, E.; Hage-Ali, M.; Hervieu, M.; Stoquert, J.P.; Studer, F.; Toulemonde, M. Track formation in SiO₂ quartz and the thermal-spike mechanism. *Phys. Rev. B* **1994**, *49*, 12457.
8. Harbsmeier, F.; Bolse, W. Ion beam induced amorphization in alpha-quartz. *J. Appl. Phys.* **1998**, *83*, 4049.
9. Ramos, S.M.M.; Clerc, C.; Canut, B.; Chaumont, J.; Toulemonde, M.; Bernas, H. Damage kinetics in MeV gold ion—Irradiated crystalline quartz. *Nucl. Instrum. Methods Phys. Res. B* **2000**, *166–167*, 31.
10. Toulemonde, M.; Ramos, S.M.M.; Bernas, H.; Clerc, C.; Canut, B.; Chaumont, J.; Trautmann, C. MeV gold irradiation induced damage in α -quartz: Competition between nuclear and electronic stopping. *Nucl. Instrum. Methods Phys. Res. Sect. B Beam Interact. Mater. At.* **2001**, *178*, 331.
11. Klaumunzer, S. Ion tracks in quartz and vitreous silica. *Nucl. Instrum. Methods Phys. Res. B* **2004**, *225*, 136.
12. Pakarinen, O.H.; Djurabekova, F.; Nordlund, K.; Kluth, P.; Ridgway, M.C. Molecular dynamics simulations of the structure of latent tracks in quartz and amorphous SiO₂. *Nucl. Instrum. Methods Phys. Res. Sect. B-Beam Interact. Mater. At.* **2009**, *267*, 1456.
13. Afra, B.; Rodriguez, M.D.; Trautmann, C.; Pakarinen, O.H.; Djurabekova, F.; Nordlund, K.; Bierschenk, T.; Giuliani, R.; Ridgway, M.C.; Rizza, G.; et al. SAXS investigations of the morphology of swift heavy ion tracks in α -quartz. *J. Phys. Condens. Matter* **2013**, *25*, 045006.
14. Leino, A.A.; Daraszewicz, S.L.; Pakarinen, O.H.; Djurabekova, F.; Nordlund, K.; Afra, B.; Kluth, P. Structural analysis of simulated swift heavy ion tracks in quartz. *Nucl. Instrum. Methods Phys. Res. Sect. B Beam Interact. Mater. At.* **2014**, *326*, 289.
15. Crespillo, M.L.; Graham, J.T.; Zhang, Y.; Weber, W.J. In-situ luminescence monitoring of ion-induced damage evolution in SiO₂ and Al₂O₃. *J. Lumin.* **2016**, *172*, 208.
16. Wesch, W.; Wendler, E. (Eds.) *Ion. Beam Modification of Solids—Ion.-Solid Interaction and Radiation Damage*; Springer International Publishing: Basel, Switzerland, 2016; Volume 61.
17. Amekura, H.; Chen, F.; Jia, Y. *Ion. Irradiation of Dielectrics for Photonic Applications*; Springer Nature: Singapore, 2020; Chapter 5.
18. Shen, H.; Brink, C.; Hvelplund, P.; Shiryaev, S.; Shi, P.; Davies, J.A. Fullerene ion (C₆₀⁺) damage in Si at 25 °C. *Nucl. Instrum. Methods Phys. Res. Sect. B Beam Interact. Mater. At.* **1997**, *129*, 203.
19. Nakajima, K.; Morita, Y.; Suzuki, M.; Narumi, K.; Saitoh, Y.; Ishikawa, N.; Hojou, K.; Tsujimoto, M.; Isoda, S.; Kimura, K. Direct observation of fine structure in ion tracks in amorphous Si₃N₄ by TEM. *Nucl. Instrum. Methods Phys. Res. Sect. B Beam Interact. Mater. At.* **2012**, *291*, 12.
20. Kitayama, T.; Morita, Y.; Nakajima, K.; Narumi, K.; Saitoh, Y.; Matsuda, M.; Sataka, M.; Tsujimoto, M.; Isoda, S.; Toulemonde, M.; et al. Formation of ion tracks in amorphous silicon nitride films with MeV C₆₀ ions. *Nucl. Instrum. Methods Phys. Res. Sect. B Beam Interact. Mater. At.* **2015**, *356–357*, 22.
21. Dunlop, A.; Jaskierowicz, G.; Della-Negra, S. Latent track formation in silicon irradiated by 30 MeV fullerenes. *Nucl. Instrum. Methods Phys. Res. Sect. B Beam Interact. Mater. At.* **1998**, *146*, 302.
22. Canut, B.; Bonardi, N.; Ramos, S.M.M.; Della-Negra, S. Latent tracks formation in silicon single crystals irradiated with fullerenes in the electronic regime. *Nucl. Instrum. Methods Phys. Res. Sect. B Beam Interact. Mater. At.* **1998**, *146*, 296.
23. Amekura, H.; Narumi, K.; Chiba, A.; Hirano, Y.; Yamada, K.; Tsuya, D.; Yamamoto, S.; Okubo, N.; Ishikawa, N.; Saitoh, Y. C₆₀ ions of 1 MeV are slow but elongate nanoparticles like swift heavy ions of hundreds MeV. *Sci. Rep.* **2019**, *9*, 14980.
24. Amekura, H.; Toulemonde, M.; Narumi, K.; Li, R.; Chiba, A.; Hirano, Y.; Yamada, K.; Yamamoto, S.; Ishikawa, N.; Okubo, N.; et al. Ion tracks in silicon formed by much lower energy deposition than the track formation threshold. *Sci. Rep.* **2021**, *11*, 185. [[PubMed](#)]
25. Lindhard, J. Influence of crystal lattice on motion of energetic charge particles. *Kgl. Danske Vidensk. Selsk. Mat.-fys. Medd.* **1965**, *34*, 1.
26. Saitoh, Y.; Chiba, A.; Narumi, K. Transmission of cluster ions through a tandem accelerator of several stripper gases. *Rev. Sci. Instrum.* **2009**, *80*, 106104. [[PubMed](#)]
27. Chiba, A.; Usui, A.; Hirano, Y.; Yamada, K.; Narumi, K.; Saitoh, Y. Novel Approaches for Intensifying Negative C₆₀ Ion Beams Using Conventional Ion Sources Installed on a Tandem Accelerator. *Quantum Beam Sci.* **2020**, *4*, 13.
28. Kluth, P.; Schnohr, C.S.; Pakarinen, O.H.; Djurabekova, F.; Sprouster, D.J.; Giuliani, R.; Ridgway, M.C.; Byrne, A.P.; Trautmann, C.; Cookson, D.J.; et al. Fine Structure in Swift Heavy Ion Tracks in Amorphous SiO₂. *Phys. Rev. Lett.* **2008**, *101*, 175503. [[PubMed](#)]
29. Bouneau, S.; Brunelle, A.; Della-Negra, S.; Depauw, J.; Jacquet, D.; Le Beyec, Y.; Pautrat, M.; Fallavier, M.; Poizat, J.C.; Andersen, H.H. Very large gold and silver sputtering yields induced by keV to MeV energy Au_n clusters (n = 1–13). *Phys. Rev. B* **2002**, *65*, 144106.
30. Ben-Hamu, D.; Baer, A.; Feldman, H.; Levin, J.; Heber, O.; Amitay, Z.; Vager, Z.; Zajfman, D. Energy loss of fast clusters through matter. *Phys. Rev. A* **1997**, *56*, 4786.
31. Ziegler, J.F.; Biersack, J.P.; Ziegler, M.D. *SRIM—The Stopping and Range of Ions in Matter*; SRIM Co.: Chester, MD, USA, 2008; Available online: <http://www.srim.org> (accessed on 6 January 2022).
32. Kaneko, T.; Saitoh, Y.; Chiba, A.; Narumi, K. *Theoretical Study on Electron-loss and Excitation in Collision of Swift MeV/atom Carbon Cluster Ions with Gases and Solids*; QST Takasaki Annual Report 2019; Takasaki Advanced Radiation Research Institute: Takasaki, Japan, 2021; p. 130.